REPORT SD-TR-89-79

Compression Phenomena in Hard-Saturated Microwave Amplifiers

S. A. MAAS
Electronics Research Laboratory
Laboratory Operations
The Aerospace Corporation
El Segundo, CA 90245

30 September 1989

Prepared for

SPACE SYSTEMS DIVISION
AIR FORCE SYSTEMS COMMAND
Los Angeles Air Force Base
P.O. Box 92960
Los Angeles, CA 90009-2960

This report was submitted by The Aerospace Corporation, El Segundo, CA 90245, under Contract No. F04701-88-C-0089 with the Space Systems Division, P.O. Box 92960, Los Angeles, CA 90009-2960. It was reviewed and approved for The Aerospace Corporation by M. J. Daugherty, Director, Electronics Research Laboratory.

Lt Steven Boyle was the project officer for the Mission-Oriented Investigation and Experimentation (MOIE) Program.

This report has been reviewed by the Public Affairs Office (PAS) and is releasable to the National Technical Information Service (NTIS). At NTIS, it will be available to the general public, including foreign nationals.

This technical report has been reviewed and is approved for publication. Publication of this report does not constitute Air Force approval of the report's findings or conclusions. It is published only for the exchange and stimulation of ideas.

Steven L. Boyle

STEVEN BOYLE, LT, USAF
MOIE Project Officer
SSD/CWHB

Raymond M. Leong

RAYMOND M. LEONG, MAJOR, USAF
MOIE Program Manager
AFSTC/WCO OL-AB

UNCLASSIFIED

SECURITY CLASSIFICATION OF THIS PAGE

REPORT DOCUMENTATION PAGE

1a REPORT SECURITY CLASSIFICATION Unclassified	1b RESTRICTIVE MARKINGS
2a SECURITY CLASSIFICATION AUTHORITY	3 DISTRIBUTION / AVAILABILITY OF REPORT Approved for public release; distribution unlimited.
2b DECLASSIFICATION / DOWNGRADING SCHEDULE	
4 PERFORMING ORGANIZATION REPORT NUMBER(S) TR-0089(4925-02)-1	5 MONITORING ORGANIZATION REPORT NUMBER(S) SD-TR-89-79
6a NAME OF PERFORMING ORGANIZATION The Aerospace Corporation Laboratory Operations 6b OFFICE SYMBOL (If applicable)	7a NAME OF MONITORING ORGANIZATION Space Systems Division
6c ADDRESS (City, State, and ZIP Code) El Segundo, CA 90245	7b ADDRESS (City, State, and ZIP Code) Los Angeles Air Force Base Los Angeles, CA 90009-2960
8a NAME OF FUNDING / SPONSORING ORGANIZATION 8b OFFICE SYMBOL (If applicable)	9 PROCUREMENT INSTRUMENT IDENTIFICATION NUMBER F04701-88-C-0089
8c ADDRESS (City, State, and ZIP Code)	10 SOURCE OF FUNDING NUMBERS PROGRAM ELEMENT NO. / PROJECT NO. / TASK NO. / WORK UNIT ACCESSION NO.

11 TITLE (Include Security Classification)

Compression Phenomena in Hard-Saturated Microwave Amplifiers

12 PERSONAL AUTHOR(S) Maas, Stephen A.

13a TYPE OF REPORT	13b TIME COVERED FROM _____ TO _____	14 DATE OF REPORT (Year, Month, Day)	15 PAGE COUNT
		1989 September 30	21

16 SUPPLEMENTARY NOTATION

17 COSATI CODES		
FIELD	GROUP	SUB-GROUP

18 SUBJECT TERMS (Continue on reverse if necessary and identify by block number)
Desensitization
Saturation
Intermodulation distortion
Volterra-series analysis
Nonlinear systems

19 ABSTRACT (Continue on reverse if necessary and identify by block number)

An earlier report from this laboratory described the anomalous compression of a weak signal by a stronger one in a hard-saturated FET amplifier. It was shown that the amplifier's compression characteristics were not consistent with the conventional theory of hard limiters. This report recasts the hard-limiter theory in terms of a Volterra series, and shows that the previously unexplained compression characteristics are to be expected in hard-saturated multistage amplifiers.

20 DISTRIBUTION / AVAILABILITY OF ABSTRACT	21 ABSTRACT SECURITY CLASSIFICATION
☒ UNCLASSIFIED/UNLIMITED ☐ SAME AS RPT ☐ DTIC USERS	Unclassified
22a NAME OF RESPONSIBLE INDIVIDUAL	22b TELEPHONE (Include Area Code) / 22c OFFICE SYMBOL

DD FORM 1473, 84 MAR 83 APR edition may be used until exhausted
All other editions are obsolete

SECURITY CLASSIFICATION OF THIS PAGE
UNCLASSIFIED

CONTENTS

FIGURES

I. INTRODUCTION

When two signals having widely different amplitudes (i.e., more than 20 dB) are applied to an ideal hard limiter, the differences in their levels increases by 6 dB. When real (i.e., nonideal) microwave FET amplifiers are used to realize limiters, however, this ideal compression characteristic is observed only when the amplifier is mildly saturated. When the amplifier is hard-saturated, the amplitude of the smaller signal often deviates substantially from its expected value. The amount of small-signal compression generally varies unpredictably with the frequency and level of the large signal. When it occurs in the front end of a receiver, this compression reduces the receiver's sensitivity to the small signal, and thus is often called desensitization.

This phenomenon has been observed experimentally in this laboratory.[1] Measurements of the compression of a small signal by a larger one were made on a commercial broadband, low-noise amplifier at frequencies near 3 GHz. Although the expected small-signal compression of 6 dB was observed under moderate levels of saturation, the small-signal level varied unpredictably when the amplifier was strongly saturated.

Because it does not conform to the conventional theory describing hard limiters, this phenomenon has heretofore been considered anomalous. However, far from being anomalous, it can be explained in a straightforward manner by means of Volterra-series theory, and is in fact the expectable consequence of saturation. It appears to be anomalous only because the ideal hard-limiter model is not adequate to describe real microwave circuits.

II. THE HARD-LIMITER MODEL

Figure 1 shows the conventional model of an ideal hard limiter. The limiter, shown schematically in Fig. 1(a), has the memoryless voltage-transfer function shown in Fig. 1(b). The limiter has no effect when the peak value of the input voltage V_i is below the threshold V_t; if $V_i > V_t$, the output voltage is clamped at V_t and includes only input frequencies (distortion components and harmonics are filtered from the output). If two signals are simultaneously applied to the limiter and one signal is much smaller than the other, the smaller signal effectively phase modulates the larger one at a rate equal to the difference of their frequencies. This case is illustrated by the diagram in Fig. 1(c), in which the output voltage V_o is described as the sum of two phasors representing the signals.

The resultant of the two phasors is

$$V_o(t) = V_1\cos[\omega_i t + \Phi\sin(\omega_m t)] \tag{1}$$

where

$$\Phi = \tan^{-1}\left(\frac{V_2}{V_1}\right) \tag{2}$$

and $\omega_m = \omega_2 - \omega_1$. When $V_2 \ll V_1$, $\Phi \approx V_2/V_1$ and Eq. (1) can be expanded to obtain

$$V_o(t) = V_1 J_0(\Phi)\sin(\omega_1 t) + V_2 J_1(\Phi)\sin[(\omega_1 + \omega_m)t] + \ldots \tag{3}$$

where J_n is the nth-order Bessel function. In the limit $V_2/V_1 \to 0$,

$$V_o(t) = V_1\left[\sin(\omega_1 t) + \frac{V_2}{2V_1}\sin(\omega_2 t) + \ldots\right] \tag{4}$$

Thus, the level of V_2 is compressed, relative to V_1, by a factor of two, or 6 dB. This degree of saturation is usually observed in practice in lightly saturated single-stage amplifiers.

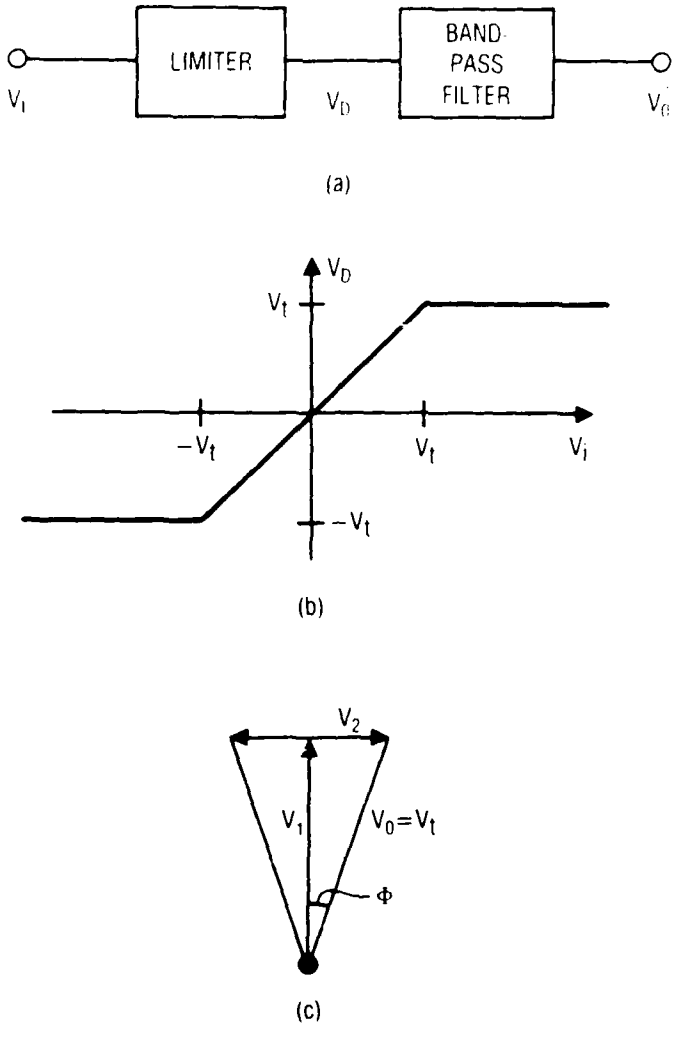

Fig. 1. The Ideal Hard Limiter. (a) The limiting section and a band-pass filter. (b) The input/output characteristic of the limiting section. (c) Phasor components of V_0 when there are two excitation components, V_1 and V_2.

III. THE VOLTERRA-SERIES MODEL

The ideal hard limiter has only a single resistive (or memoryless) nonlinearity, and has no feedback. Real amplifiers have both linear and nonlinear reactances, feedback, and possibly even multiple memoryless nonlinearities; the most significant of the latter are the transistor's transconductances.

The output $V_o(t)$ of a nonlinear system having both reactive and resistive nonlinearities can be expressed by the frequency-domain form of the Volterra series:

$$V_o(t) = \sum_{n=1}^{N} \frac{1}{2^n} \sum_{q1=-Q}^{Q} \sum_{q2=-Q}^{Q} \cdots \sum_{qn=-Q}^{Q} V_{s,q1} V_{s,q2} \cdots V_{s,qn} H_n(\omega_{q1}, \omega_{q2} \cdots \omega_{qn}) \exp[\omega_{q1} + \omega_{q2} + \cdots \omega_{qn})t] \quad (5)$$

in which the excitation $V_i(t)$ consists of Q noncommensurate sinusoids, and can be expressed as

$$V_i(t) = \frac{1}{2} \sum_{q=-Q}^{Q} V_q \exp(j\omega_q t) \quad (6)$$

We note that $\omega_{-q} \equiv -\omega_q$ in Eq. (6). The complex quantity $H_n(\omega_{q1}, \omega_{q2} \cdots \omega_{qn})$ is called the nth-order nonlinear transfer function, or the nth-order Volterra kernel of the system. Analogous to the transfer function of a linear system, it relates the nth-order response at the frequency $\omega_{q1} + \omega_{q2} + \cdots \omega_{qn}$ to the individual excitation tones [the first-order term $H_1(\omega_q)$ is in fact the linear transfer function of the system]. The sum of these responses, at all possible orders and mixing frequencies, is the total response of the system. Thus, Eq. (5) represents the sum of a

very large number of frequency components, each of which occurs at a frequency that is the linear combination of a set of n excitation frequencies. These frequencies are called nth-order mixing frequencies.

A careful examination of Eq. (5) shows that many mixing frequencies of different orders are identical. For example, when the excitation has two tones (Q = 2), the third-order (n = 3) output includes terms at $\omega_1 + \omega_{-1} + \omega_1 = \omega_1$ and $\omega_1 + \omega_{-1} + \omega_2 = \omega_2$. Although these components occur at excitation frequencies, they are still third-order mixing frequencies, and because H_3 is complex, they may have phases that are different from those of the linear outputs. Mixing frequencies equal to the excitation frequencies occur in all odd-order terms of Eq. (5).

We now consider the case of a nonlinear system having two excitation tones, one at ω_1 that is very strong and another at ω_2 that is much weaker. From Eq. (5) we find that the outputs at ω_1 and ω_2 can be expressed, respectively, as

$$\begin{aligned} V_o(\omega_1) \approx\ & V_1 H_1(\omega_2) + (3/4)V_1^3 H_3(-\omega_1, \omega_1, \omega_1) \\ & + (5/8)V_1^5 H_5(-\omega_1, -\omega_1, \omega_1, \omega_1, \omega_1) \\ & + (35/64)V_1^7 H_7(-\omega_1, -\omega_1, -\omega_1, \omega_1, \omega_1, \omega_1, \omega_1) \\ & + \ldots \end{aligned} \tag{7}$$

and

$$\begin{aligned} V_o(\omega_2) \approx\ & V_2 H_1(\omega_2) + (3/2)V_1^2 V_2 H_3(-\omega_1, \omega_1, \omega_2) \\ & + (15/8)V_1^4 V_2 H_5(-\omega_1, -\omega_1, \omega_1, \omega_1, \omega_2) \\ & + 35/16)V_1^6 V_2 H_7(-\omega_1, -\omega_1, -\omega_1, \omega_1, \omega_1, \omega_1, \omega_2) \\ & + \ldots \end{aligned} \tag{8}$$

Equations (7) and (8) are approximate; many terms in Eq. (5) that contribute to $_{o}(\omega_1)$ and $V_o(\omega_2)$ are negligible when $V_2 \ll V_1$, and these terms have not been included.

Each of the additive terms in Eqs. (7) and (8) can be represented by a phasor. Without loss of generality, we can assume V_1 and V_2 to be real; then the magnitude of each phasor is proportional to the appropriate product of the excitation-voltage components, and the phase of each phasor is equal to the phase of H_n. Note that the H_n in Eqs. (7) and (8) are not identical; consequently, their magnitudes and phases are, in general, different.

IV. THE IDEAL HARD LIMITER DESCRIBED BY THE VOLTERRA-SERIES MODEL

Because its transfer function has discontinuous derivatives near the saturation point, the ideal hard limiter cannot be described by a Volterra-series formulation. However, if we replace this transfer function with a memoryless one that has continuous derivatives, the Volterra series is applicable. We therefore approximate the limiter characteristic as shown in Fig. 2; we derived the approximate curve by fitting a polynomial to the function $V_o = \tanh(V_i)$ in the range $V_i = (-5,5)$. The resulting polynomial is

$$V_o = a_1 V_i + a_3 V_i^3 + a_5 V_i^5 + a_7 V_i^7 + \ldots \qquad (9)$$

where

$$a_1 = 0.8454$$

$$a_3 = -0.10703$$

$$a_5 = 6.407 \cdot 10^{-3}$$

$$a_7 = -1.264 \cdot 10^{-5}$$

In the following calculations this polynomial will be truncated after the seventh-degree term. The nonlinear transfer functions H_n can be found by means of the probing method.[2,3] We find that in both Eqs. (7) and (8), $H_n = a_n$; i.e., the power-series coefficients are the Volterra kernels. Thus, in this case the H_n are all real and have phases of either 180 or 0 degrees. We note that a symmetrical, odd, monotonic function such as that shown in Fig. 2 will always have $a_1, a_5, a_9 \ldots > 0$ and $a_3, a_7, a_{11} \ldots < 0$, and $a_n = 0$ when n is even. Also, because Eq. (9) is valid only in the range $V_i = (-5,5)$, we should expect the Volterra series to be accurate only within, at most, this same range.

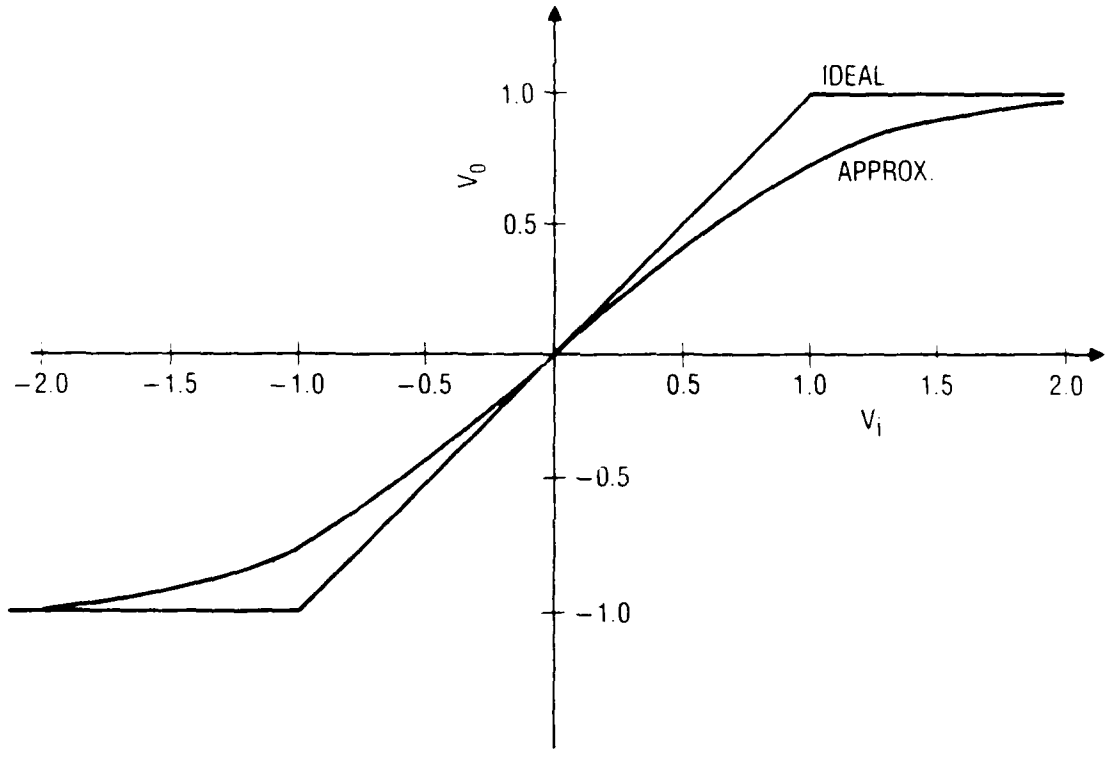

Fig. 2. Characteristics of the Ideal and the Approximate Limiter

Figure 3 shows a phasor diagram representing either Eq. (7) or (8), in which the output voltage $V_o(\omega)$ is the vector sum of the phasors representing the individual terms of those equations. [Note that this diagram does not illustrate the same phenomenon as does Fig. 1(c); the Volterra-series terms in Fig. 3 represent components of the same signal, and are all at the same frequency; Fig. 1(c) shows two separate signals at different frequencies.] When V_1 is small, as shown in Fig. 3(a), the higher-order terms are negligible and only a single term, the linear one (n = 1, containing H_1) is significant. However, as V_1 increases, the third-order term increases rapidly. Because the phase of H_3 in an ideal hard limiter is 180 degrees, the sum of the first- and third-order phasors does not increase as rapidly as the first-order term, and thus the output level begins to saturate; this situation is illustrated in Fig. 3(b).

If only first- and third-order terms existed, increasing V_1 further would eventually cause $V_o(\omega)$ to peak and then decrease. However, before the output level can decrease, the fifth-order term becomes significant; because its phase is zero, it adds a positive component to $V_o(\omega)$ that opposes the negative third-order term and thus prevents $V_o(\omega)$ from decreasing. As V_1 is increased, subsequent higher-order terms become progressively more significant in this manner, and as a result the limiter has a smooth output-saturation characteristic. Figure 3(c) shows the phasors when the limiter is strongly saturated.

It is possible to illustrate the compression of $V_o(\omega_2)$ by dividing Eq. (8) by Eq. (7) and substituting a_n for H_n. The result can be expressed as

$$\frac{V_o(\omega_2)}{V_o(\omega_1)} = \frac{V_2}{V_1} \frac{a V_1 + 2b V_1^3 + 3c V_1^5 + 4d V_1^7 + \ldots}{a V_1 + b V_1^3 + c V_1^5 + d V_1^7 + \ldots} \qquad (10)$$

where $a = a_1$, $b = 0.75a_3$, $c = 0.625a_5$, and $d = 0.5469a_7$. This ratio becomes infinite as $V_1 \to \infty$, and thus appears to predict the unlimited expansion (instead of the compression) of V_2 with V_1. However, because of the truncation of the Volterra series in Eqs. (7) and (8), and because

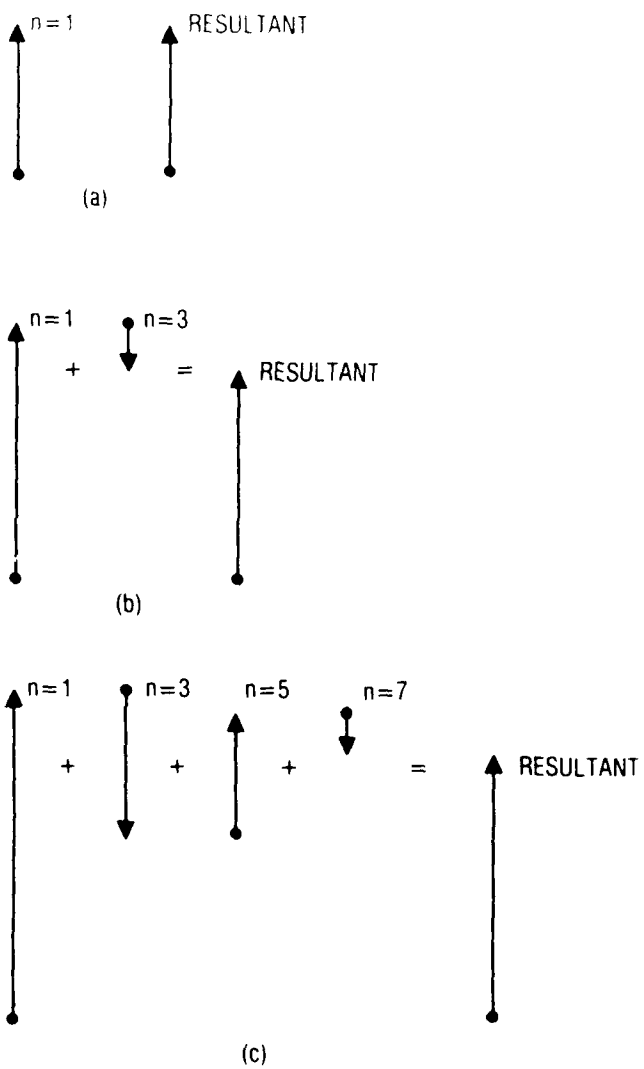

Fig. 3. Phasor Representations of the Voltage Components at the Output of the Limiter at Either ω_1 or ω_2 (the phasors are drawn separately for clarity). (a) $V_i' << V_t'$; (b) $V_i \approx V_t$; (c) $V_i >> V_t$.

Eq. (9) is valid only within the range $V_i = (-5,5)$, Eq. (10) is not valid at large values of V_1. Figure 4 shows a plot of Eq. (10) as a function of V_1; it indicates that $V_o(\omega_2)/V_o(\omega_1)$ is compressed to a value of $0.43V_2/V_1$ when $V_1 \gg 1$; this result is in reasonable agreement with conventional theory, which predicts a compression value of $0.5V_2/V_1$. The difference is probably due to the truncation of the series after only the seventh degree, and may also be related to approximations inherent in the hard-limiter theory.

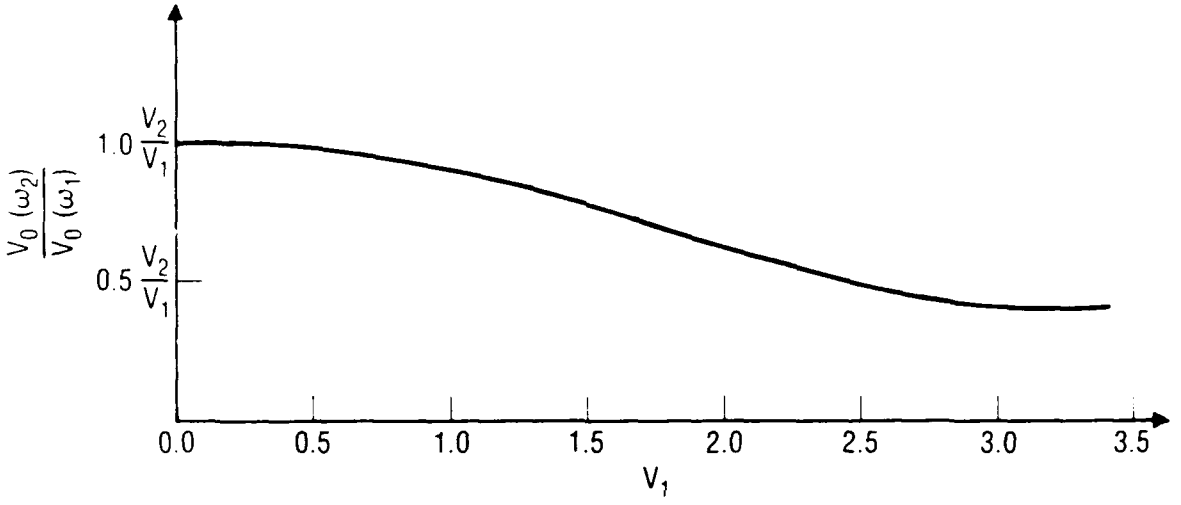

Fig. 4. The Compression of $V_0(\omega_2)$ by V_1 (calculated by means of the Volterra-series model)

V. COMPRESSION IN REAL AMPLIFIERS

The analysis of a real amplifier differs from that of the ideal limiter in two respects. First, a single amplifier stage has reactive as well as resistive (memoryless) nonlinearities, which may include feedback resulting from the transistor's nonlinear reverse-transfer capacitance. These properties affect the nonlinear transfer functions -- especially those of the highest order -- in a manner that is generally unpredictable. Second, in a multistage amplifier more than one stage can saturate if the input level is very great. The input to the final stage may then consist not only of voltage components at the original input frequencies, but also of harmonics and intermodulation products generated in earlier stages. Thus, even if the input signal consists of only two tones, the signal entering the final stage may consist of a multiplicity of tones, not just two. Because of the many possible interactions between these components, the phases and magnitudes of the nonlinear transfer functions of a multistage amplifier can vary substantially with small changes in power level and frequency.

Figure 5 shows a phasor diagram of one possible set of voltage components in a real amplifier. Because the reactive nonlinearities arise in the transistor's parasitic capacitances and are therefore relatively small, the lower-order transfer functions are dominated by memoryless nonlinearities, especially the transconductance. However, the higher-order transfer functions often include high-frequency terms, and thus are more strongly affected by small reactive nonlinearities. These are the terms that dominate at high levels of V_1. Consequently, at moderate levels of saturation the magnitude of the resultant phasor representing $V_o(\omega_2)$ varies approximately in accordance with hard-limiter theory. However, under heavy saturation $V_o(\omega_2)$ varies apparently randomly with changes in signal level and frequency; under some conditions it can even disappear completely. It is important to note that saturation changes not only the amplitude of $V_o(\omega)$ but also its phase.

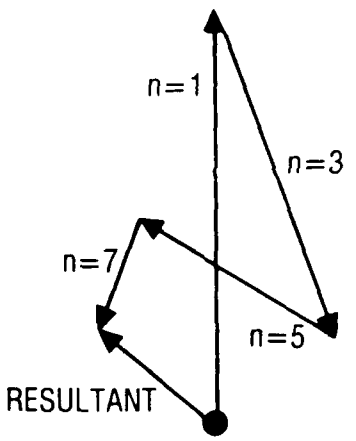

Fig. 5. One Possible Set of Voltage-Component Phasors at the Output of a Strongly Saturated Real Amplifier

Because the unpredictable compression of $V_o(\omega_2)$ is the result of higher-order nonlinear transfer functions, and these are dominated by strong nonlinearities and high mixing frequencies, it may be possible to improve the compression characteristics of practical amplifiers by minimizing the effects of these nonlinearities. For example, designing a transistor's matching circuits to reject harmonics and high-frequency mixing products, as well as to short-circuit the gate drain of a FET (or the base and collector of a bipolar transistor) at out-of-band frequencies, may improve the amplifier's saturation characteristics. It may also be helpful to include bandpass filters between the stages of multistage amplifiers, or at least between the last two or three stages. Minimizing nonlinearities inherent in the FET by employing a graded channel-doping profile may also help. Finally, using a bias circuit having a low source impedance and a high current capability may reduce saturation effects associated with inadequate bias power. It is difficult to predict theoretically which factors dominate in creating well-behaved higher-order transfer functions; thus, the task of improving the saturation performance of amplifiers is best approached experimentally.

VI. REFERENCES

1. K. H. Hurlbut, W. A. Johnson, and T. T. Mori, "Nonlinear Behavior of Receiver Preamplifiers," Aerospace Corp. Technical Memorandum No. ATM-83(3907)-8 (19 May 1983).

2. D. D. Weiner and J. F. Spina, Sinusoidal Analysis and Modeling of Weakly Nonlinear Circuits (Van Nostrand: New York, 1980).

3. S. A. Maas, Nonlinear Microwave Circuits (Artech House: Norwood, Mass., 1988).

LABORATORY OPERATIONS

The Aerospace Corporation functions as an "architect-engineer" for national security projects, specializing in advanced military space systems. Providing research support, the corporation's Laboratory Operations conducts experimental and theoretical investigations that focus on the application of scientific and technical advances to such systems. Vital to the success of these investigations is the technical staff's wide-ranging expertise and its ability to stay current with new developments. This expertise is enhanced by a research program aimed at dealing with the many problems associated with rapidly evolving space systems. Contributing their capabilities to the research effort are these individual laboratories:

Aerophysics Laboratory: Launch vehicle and reentry fluid mechanics, heat transfer and flight dynamics; chemical and electric propulsion, propellant chemistry, chemical dynamics, environmental chemistry, trace detection; spacecraft structural mechanics, contamination, thermal and structural control; high temperature thermomechanics, gas kinetics and radiation; cw and pulsed chemical and excimer laser development including chemical kinetics, spectroscopy, optical resonators, beam control, atmospheric propagation, laser effects and countermeasures.

Chemistry and Physics Laboratory: Atmospheric chemical reactions, atmospheric optics, light scattering, state-specific chemical reactions and radiative signatures of missile plumes, sensor out-of-field-of-view rejection, applied laser spectroscopy, laser chemistry, laser optoelectronics, solar cell physics, battery electrochemistry, space vacuum and radiation effects on materials, lubrication and surface phenomena, thermionic emission, photosensitive materials and detectors, atomic frequency standards, and environmental chemistry.

Computer Science Laboratory: Program verification, program translation, performance-sensitive system design, distributed architectures for spaceborne computers, fault-tolerant computer systems, artificial intelligence, microelectronics applications, communication protocols, and computer security.

Electronics Research Laboratory: Microelectronics, solid-state device physics, compound semiconductors, radiation hardening; electro-optics, quantum electronics, solid-state lasers, optical propagation and communications; microwave semiconductor devices, microwave/millimeter wave measurements, diagnostics and radiometry, microwave/millimeter wave thermionic devices; atomic time and frequency standards; antennas, rf systems, electromagnetic propagation phenomena, space communication systems.

Materials Sciences Laboratory: Development of new materials: metals, alloys, ceramics, polymers and their composites, and new forms of carbon; nondestructive evaluation, component failure analysis and reliability; fracture mechanics and stress corrosion; analysis and evaluation of materials at cryogenic and elevated temperatures as well as in space and enemy-induced environments.

Space Sciences Laboratory: Magnetospheric, auroral and cosmic ray physics, wave-particle interactions, magnetospheric plasma waves; atmospheric and ionospheric physics, density and composition of the upper atmosphere, remote sensing using atmospheric radiation; solar physics, infrared astronomy, infrared signature analysis; effects of solar activity, magnetic storms and nuclear explosions on the earth's atmosphere, ionosphere and magnetosphere; effects of electromagnetic and particulate radiations on space systems; space instrumentation.